Turbulence Structure in a Shock Wave/Turbulent Boundary-Layer Interaction

M. S. Selig*
Pennsylvania State University, University Park, Pennsylvania
J. Andreopoulos†
City College of the City University of New York, New York, New York
K. C. Muck‡
National Bureau of Standards, Gaithersburg, Maryland
J. P. Dussauge§
Institute Mécanique Statistique de la Turbulence, Marseille, France
and
A. J. Smits¶
Princeton University, Princeton, New Jersey

The boundary-layer turbulence structure in a two-dimensional 24-deg compression corner flow was investigated experimentally in the Princeton University 203 × 203-mm supersonic blowdown wind tunnel. The incoming conditions were $M_\infty = 2.84$, $Re_\infty/l = 6.5 \times 10^7$, and $\delta_0 = 26$ mm. The results show that the maximum mass-flux turbulence intensity is amplified by a factor of about 5, whereas the mean mass flux increases by only 2 through compression. Probability density functions (pfd's) of the mass-flux fluctuations show that upstream the distributions are Gaussian-like and typical of a fully turbulent boundary layer. Behind the interaction, however, the distributions are bimodal, centering about a level indicative of the freestream mass flux and a lower level indicative of the mass flux near the wall. The unsteady shock motion does not appear to contribute signficantly to the turbulence amplification. It is suggested that the strong, bimodal mixing indicated in the pdf's is probably caused by the presence of large-scale motions associated with the instability of the inflectional velocity profiles observed downstream of the interaction. Space-time correlations of the mass flux and wall pressure were measured, as well as the level of intermittency of the boundary layer to further characterize the changes in the boundary-layer structure through the interaction.

Nomenclature

C_f = skin-friction coefficient
f = frequency
K_1, K_2 = constants used for intermittency calculation
l = length
M = Mach number
$\langle (P)' \rangle$ = rms value
$(\bar{P})$ = long-time average
$(P)'$ = fluctuating quantity
p = wall pressure
Re = Reynolds number
t, T = time
T_0 = stagnation temperature
U = velocity
x = distance from corner (positive downstream)
y = normal distance from wall (both upstream and downstream)
δ_0 = boundary-layer thickness
δ^* = displacement thickness
θ = momentum thickness
ρ = fluid density
σ = short-time variance
σ_0 = short-time variance above the boundary layer
τ = time delay
Φ = power spectrum ($f \times$ energy spectrum)
Ω = boundary-layer intermittency

Subscripts
∞ = freestream condition
0 = stagnation condition
p = location of wall-pressure measurement
δ_0 = based on the boundary-layer thickness
ρU = location of mass-flux measurement

Presented as Paper 87-0550 at the AIAA 25th Aerospace Sciences Meeting, Reno, NV, Jan. 12–15, 1987; received April 13, 1987; revision received July 8, 1988.

*Graduate Student. Student Member AIAA.
†Associate Professor. Member AIAA.
‡Research Engineer. Member AIAA.
§Member AIAA.
¶Associate Professor. Member AIAA.

I. Introduction

THE interaction between a shock wave and a turbulent boundary layer arises in many practical flows and therefore continues to be the subject of considerable research. Despite this attention, much remains to be understood about these complex interactions, especially for flows with boundary-layer separation. Experimental studies mostly have reported the mean-flow properties. More recently, however, researchers have begun to examine the detailed time-dependent nature of these flows. This shift of emphasis comes not only from recent developments in high-frequency measurements but also from the recognized deficiencies in the current state of turbulence modeling for supersonic turbulent boundary layers. While it is realized that conventional turbulence models can predict attached flows reasonably well, it is also clear that

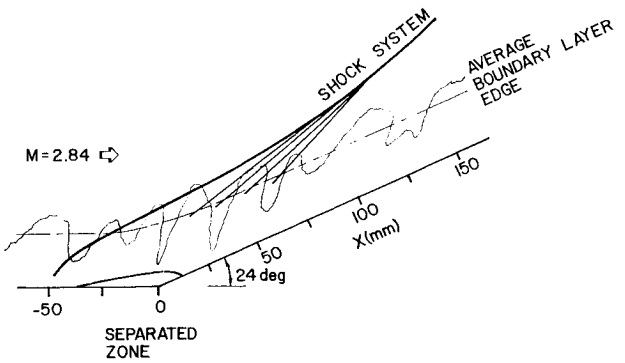

Fig. 1 Mach 3, 24-deg compression corner mean flowfield model adapted from Settles et al.[21]

extrapolation of these methods to flows with separation has not been satisfactory.[1-4] This lack of success has provided the impetus for detailed experiments of shock wave/turbulent boundary-layer interactions in an effort to develop a better understanding of these complex flows.

The present investigation considers a separated flow over a two-dimensional 24-deg compression corner at Mach 2.84 as shown in Fig. 1. From previous experiments[5-9] much already is known about this particular flow. Shock-induced separation[5] along with large-scale shock oscillation creates a highly unsteady flow.[6,7] Shadowgrams appeared to show that the shock near the wall was composed of many subsidiary shocks. It has since, however, been shown that the illusion is caused by spatial integration of a single shock that wrinkles randomly in the spanwise direction with a wavelength less than δ_0.[6,8] This wrinkling appears at a given spanwise position as a streamwise oscillation with an amplitude of order δ_0 at frequencies around 2 kHz.[9] The cause for this type of shock instability has been examined by a number of reachers and still remains at issue. It seems reasonable to suppose that the unsteadiness is related to the large-scale boundary-layer structures that convect into the shock from upstream,[8,9] and that it is connected with the instantaneous behavior of the separated zone.[10]

Previous studies of compression corner flows have demonstrated the dramatic turbulence amplification that takes place as the incoming layer passes through the interaction (see, for example, Smits and Muck[11]). In addition, Ardonceau[12] and Ardonceau et al.[13] found for a Mach 2.25, 18-deg compression corner flow with separation that a significant amount of energy was contained in large-scale structures that passed through the shock. Interestingly, spanwise statistics suggested that contrarotating vortices of the Taylor-Görtler type may emanate from the corner region.[8,12] This same phenomenon was believed to be present in a Mach 2.46 reattaching free shear layer.[14]

The previous studies of the 24-deg compression corner flowfield have been confined to investigations of the shock motion using wall-pressure transducers in the regions upstream or in the vicinity of the corner, leaving the downstream characteristics of the flow essentially unexamined. In the present study, we focus our attention on the unsteady aspects of the shock wave and its influence on the turbulence structure of the downstream boundary layer.

Experimental Facility, Test Conditions, and Instrumentation

The experiment was performed in the Princeton University 203 × 203 mm (8 × 8 in.), Mach 3 blowdown wind tunnel as shown in Fig. 2. The incoming floor boundary layer made a natural transition to turbulence in the nozzle and developed along the approximately adiabatic wall of the tunnel. At the location of the compression corner (1.95 m downstream of the nozzle throat), the boundary layer was typical of a zero-pressure gradient, fully turbulent boundary layer in equilibrium, and it obeyed both the law of the wake and law of the wall.[5,15]

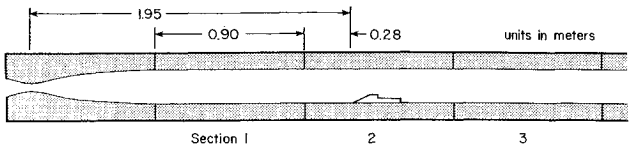

Fig. 2 Princeton University Gas Dynamics Laboratory Mach 3 supersonic blowdown facility.

Table 1 Boundary-layer characteristics and incoming flow conditions

Test conditions
$p_0 = 0.69 \times 10^6$Pa (100 psi)
$T_0 = 270$ K
$M_\infty = 2.84$
$Re_\infty/l = 6.5 \times 10^7$/m
$\delta_0 = 26$ mm
$\delta^* = 6.4$ mm
$\theta_0 = 1.3$ mm
$C_{f0} = 0.00115$

Its mean flow characteristics are summarized in Table 1. For these conditions, the freestream turbulence level based on the mass-flux fluctuations has been recorded at 1-1.5%.[16] The 24-deg compression corner model was 292.1 mm long, 41.4 mm high, and 152.4 mm wide. To improve the flowfield two-dimensionality, 6.4-mm-thick aerodynamic fences with a 30-deg bevel were screwed to the sides of the model. With the fences installed, the spacing between the model and the tunnel sidewall was enough (18.9 mm) to allow the sidewall boundary layer to pass by with a minimum of interference.

Measurements of the fluctuating wall static pressure along the tunnel centerline were made using miniature differential pressure transducers manufactured by Kulite Semiconductor Inc. (Model XCQ-062-25-D). The pressure sensitive diaphragm is 0.7 mm in diameter and has a natural frequency of 500 kHz, as quoted by the manufacturer. Since the diaphragm is recessed 1.9 mm beneath the protective screen (which is mounted flush with the tunnel floor), a standing pressure wave in the 60-80 kHz frequency range is excited between the diaphragm and the screen. Consequently, the frequency range is limited to frequencies below approximately 60 kHz. This usable frequency range is suitable because the pressure transducers are used mainly to detect the low-frequency shock motion.

The constant-temperature hot-wire technique of Smits et al.[17] was used to measure the mass-flux fluctuations. The hot wires were made at the Princeton Gas Dynamics Laboratory. The active element of the hot wire, the part sensitive to the mass flux, was 0.8-1.0 mm long. Only hot wires with a frequency response better than 100 kHz were used, provided that they did not "strain-gage," a term that refers to the high-frequency resonances that are often observed during hot-wire operation in supersonic flows.[18]

The high-frequency wall-pressure and mass-flux signals were amplified, filtered, and digitally sampled at frequencies up to 1 MHz using a CAMAC TD8210 Waveform Analyzer. Mean flow quantities were taken at a slower sampling rate using a Preston Scientific GMAD-4 A/D converter. The data were recorded on magnetic tapes for later data reduction, which included statistical analysis, spectral analysis of the fluctuating signals, as well as space-time correlations of the wall pressure and mass flux upstream and downstream of the corner. More details of the experimental procedure were given by Selig.[19]

Results and Discussion

Settles[20] was the first to examine this 24-deg compression corner flow as part of a broad mean-flow survey involving

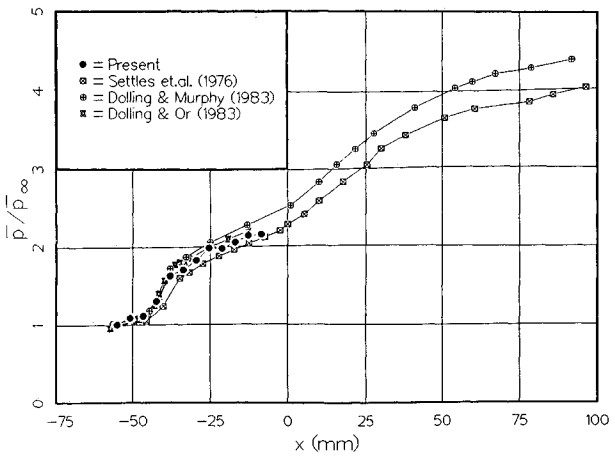

Fig. 3 Mean wall-pressure distribution compared with the measurements of Settles et al.,[5] Dolling and Murphy,[6] and Dolling and Or.[7]

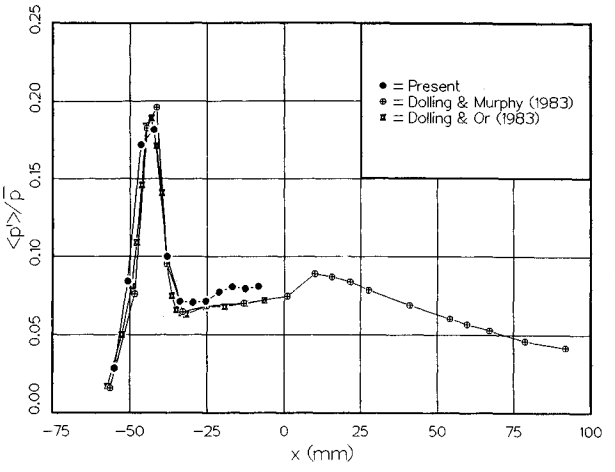

Fig. 4 Rms wall-pressure distribution compared with the measurements of Dolling and Murphy[6] and Dolling and Or.[7]

several compression corner flows. Of all the two-dimensional cases studied by Settles, the 24-deg compression corner flow was extensively surveyed primarily because it displayed a large region of shock-induced separation, as shown in the mean-flow model given in Fig. 1. The boundary layer was found to separate (in the mean) at $x = -34$ mm and reattach at $x = 11$ mm, and the maximum height of the separation bubble was about 6 mm for a boundary-layer thickness of 26 mm. It should be noted that a variety of boundary-layer thicknesses have been used for the same flow studied here. For example, Settles[20] found $\delta_0 = 21$ mm and later changed to $\delta_0 = 23$ mm.[21] More recently, boundary-layer thicknesses of 22, 24, and 28 mm were used.[6,8,22] These differences reflect not so much a slight change of conditions as a change of opinion as to how the boundary-layer thickness should be calculated from experimental measurements. As pointed out by Fernholz and Finley,[23] estimates of the boundary-layer thickness in a compressible turbulent boundary layer can be ambiguous, and it is preferable to use an integral thickness such as the momentum or displacement thickness as the nondimensionalizing length scale. In some cases, the parameter $Re^a_{\delta_0}/\delta_0$ has been used for scaling in two-dimensional shock wave/turbulent boundary layers.[24] In rapidly distorted flows, however, it is not clear that any one length scale is useful for scaling purposes, and, to avoid further confusion, all lengths will be reported without nondimensionalization.

Wall-Pressure Distribution

The wall-pressure distribution between $x = -8.5$ and -55.0 mm was measured upstream of the corner with a 4.2-mm spacing between pressure transducers. The mean wall-pressure distribution normalized by the freestream static pressure is shown in Fig. 3, where it is compared with earlier measurements.[5-7] Given that the flow is nominally two-dimensional, the discrepancies are probably within experimental error. We now know that the initial mean pressure rise is produced by the unsteady shock that oscillates with an amplitude of order δ_0; it is the average of the undisturbed pressure upstream of the moving shock and the higher pressure behind the shock. With this view, a higher mean pressure indicates that the shock spends more time upstream of that station than a station with a lower mean pressure. As a result, the rms values of the wall-pressure fluctuations reaches a peak just upstream of the mean separation point ($x = -34$ mm). The rms values of the wall-pressure fluctuations are presented in Fig. 4, and these results compare very well with earlier data.[6,7]

The energy spectra of the wall pressure nondimensionalized by the square of the local mean pressure is shown in Fig. 5. When plotted in this form (linear-log), the spectra clearly show the frequencies of the wall pressure that contribute most to the rms wall-pressure fluctuations shown in Fig. 4. Note that the

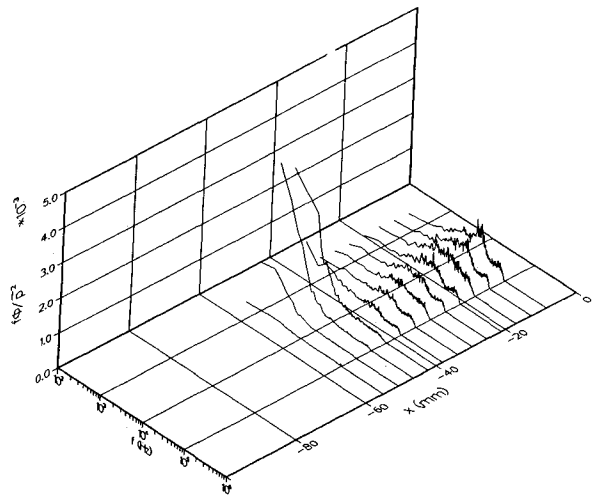

Fig. 5 Energy spectra of the wall-pressure upstream of the corner.

small rise in the spectra between 60 and 80 kHz is nonflow-related and comes from the resonance of the transducer as previously discussed. Between $x = -34$ and -55 mm, the wall-pressure fluctuations are clearly dominated by the broadband low-frequency oscillations of the shock. As discussed in previous studies, the shock is known to oscillate randomly at frequencies below 5 kHz, with a mean between 1.5-2 kHz,[6] although the distribution is highly skewed and extends up to a frequency of 10 kHz.[9] Fluctuations at frequencies higher than 10 kHz are caused purely by turbulent fluctuations, although below this frequency there is an overlap between frequencies associated with turbulence and with shock motion. One might expect that the low-frequency shock unsteadiness would produce low-frequency pressure fluctuations that would convect downstream into the separated corner region. On the contrary, immediately behind the shock the low-frequency fluctuations are small compared with the high-frequency fluctuations that grow in strength toward the corner.

Mass-Flux Turbulence Intensity Profiles

As the boundary layer passes through the unsteady shock wave and subsequently turns through 24 deg, the amplification of the mass-flux fluctuations is dramatic. To show this effect, four mass-flux turbulence intensity profiles, one upstream and three downstream of the interaction, are shown in Fig. 6. Although the compression increases the freestream mass flux by a factor of 2.0, the maximum turbulence intensity in the downstream boundary layer ($x = 101.6$ mm, not shown) increases to 4.8 times that of the maximum turbulence intensity upstream of the interaction ($x = -95.4$ mm). In Fig. 7, the

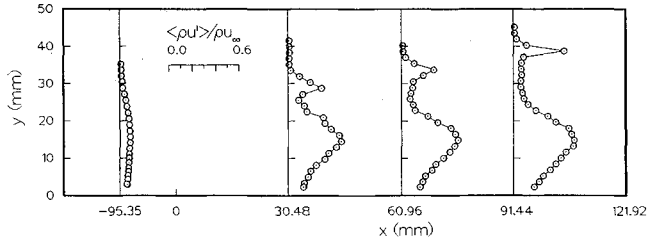

Fig. 6 Upstream and downstream mass-flux turbulence intensity profiles.

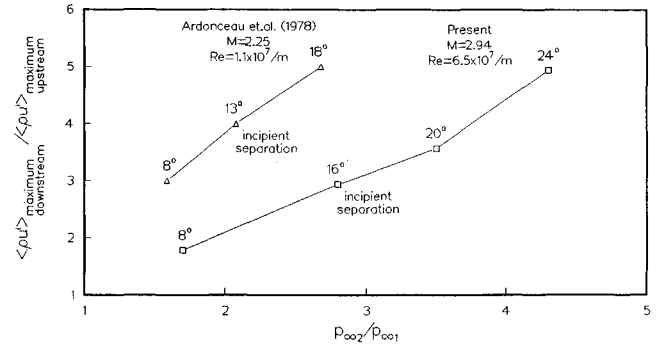

Fig. 7 Maximum turbulence intensity ratio of the upstream to downstream mass flux plotted against the inviscid pressure rise for the present 24-deg case and the 8, 16, and 20-deg cases of Smits and Muck,[11] and the 8, 13, and 18-deg cases of Ardonceau et al.[13]

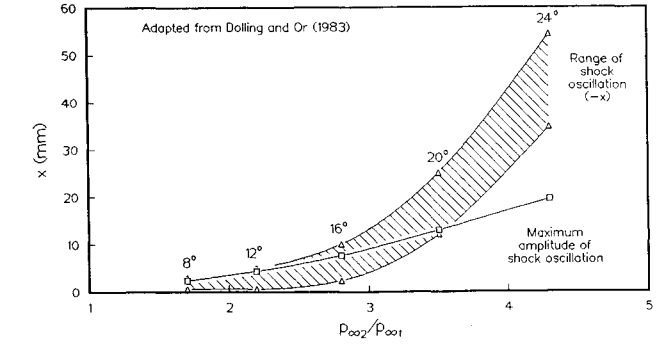

Fig. 8 Range and amplitude of the shock oscillation for the five compression corners examined by Dolling and Or.[7]

maximum turbulence intensity ratio (using $x = 101.6$ mm as the downstream location) is plotted against the inviscid pressure rise for the present 24-deg case along with the 8, 16, and 20-deg cases studied by Smits and Muck.[11] Ardonceau[12] made mass-flux measurements by hot-wire anemometry in a $M_\infty = 2.25$, $Re_\infty/l = 1.1 \times 10^7$/m flow over 8, 13, and 18-deg compression corners corresponding to attached, incipiently separated, and separated flows, respectively. His results are plotted in Fig. 7 to show the same trend of increasing turbulence intensity with shock strength. The LDV measurements of Kuntz et al.[25] in a $M_\infty = 2.94$ flow over 8, 12, 16, 20, and 24-deg compression corners also display the same trend.

Figure 8 shows the maximum amplitude of the unsteady shock and the range of the unsteady shock motion at the wall vs the inviscid pressure rise for the 8, 12, 16, 20, and 24-deg cases as determined from the data of Dolling and Or.[7] The furthest downstream point of the range of movement of the unsteady shock motion closely coincides with the mean separation line as determined from surface flow visualization, and it will be considered as the separation point for the sake of argument. The almost linear growth of both the maximum turbulence intensity ratio and the maximum amplitude of the unsteady shock motion with pressure rise appears to be in agreement with the conclusions of Refs. 26 and 27 that the

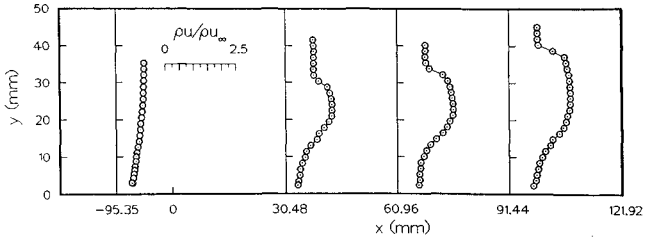

Fig. 9 Upstream and downstream mean mass-flux profiles.

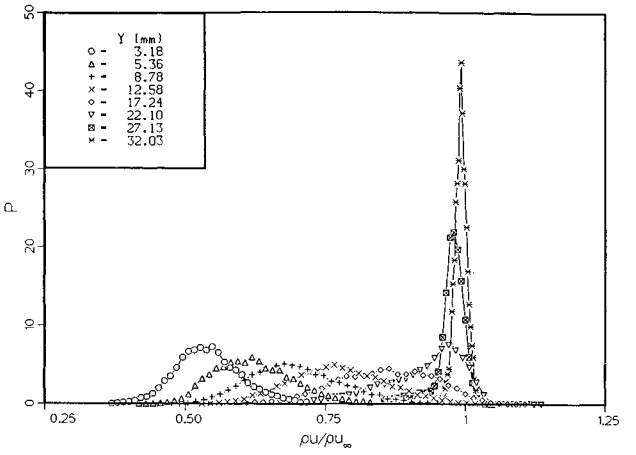

Fig. 10 Probability density functions of the upstream mass-flux profile ($x = -95.4$ mm).

increase in turbulence activity is related to the increasing shock oscillation. More will be given on this point later. However, from Fig. 8, it is clear that the turbulence amplification is not closely related to the size of the separated region; for angles less than 16 deg there is no separated region at all.

The downstream turbulence intensity profiles show two peaks (see Fig. 6). The relatively narrow peak outside the boundary layer occurs in the unsteady shock region and should be considered as "false" turbulence since it is produced by the mass-flux jumps across the unsteady shock. The second peak is much broader and is located near the middle of the boundary layer. Figure 9 shows the mean mass-flux profiles for the same x stations used in Fig. 6. Interestingly, Figs. 6 and 9 show that the peak in the turbulence intensity and the inflection point in the mean mass-flux profile happen at approximately the same distance from the wall.

Even more interesting information can be derived from the probability density functions (pdf's) of the upstream and downstream mass flux shown in Figs. 10 and 11. The upstream pdf's (Fig. 10) show, as one might expect, Gaussian-like distributions with a mean that gradually increases up through the boundary layer. In sharp contrast, the downstream pdf's (Fig. 11) center around two distinct mass-flux levels. Referring to Fig. 11, the mass flux begins to center around $0.75\rho U_\infty$ for $y < 11.7$ mm, and for $y > 18.1$ mm the mass flux centers around $2.2\rho U_\infty$, which represents the freestream value downstream of the interaction. Between $y = 11.7$ and 18.1 mm, the pdf's are bimodal, and here the turbulence intensities are largest. Apparently, the mass flux fluctuates between two distinct levels, one level representative of the freestream behind the shock and another level representative of the flow very near the wall. The pdf's for $x = 30.5$ and 61.0 mm show the same bimodal shape with the peaks shifted to slightly lower values closer to the corner. A similar bimodal pdf shape was found in studying a compressible reattaching shear layer.[28]

Two feasible explanations for this behavior can be provided. First, Taylor-Görtler vortices have been suspected to occur in this type of flow with concave curvature,[8,12,14] and this mechanism may be important here. Unsteady contrarotating vor-

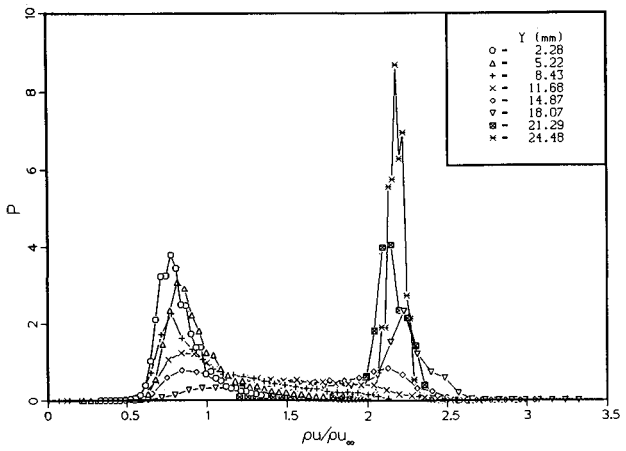

Fig. 11. Probability density functions of the downstream mass-flux profile (x = × 91.4 mm).

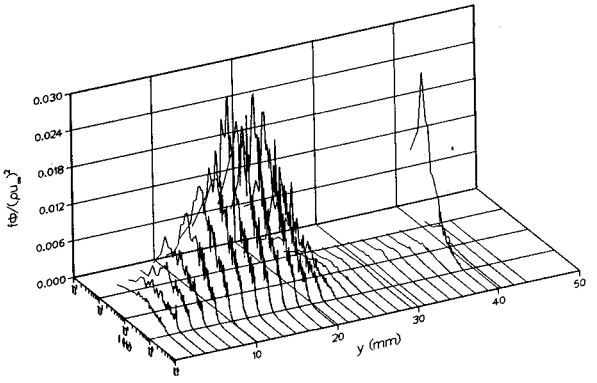

Fig. 12. Energy spectra of the dowstream mass-flux profile (x = 91.4 mm).

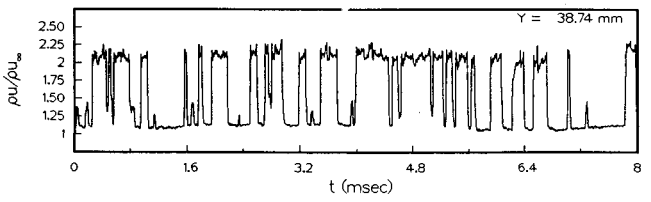

Fig. 13 Time history of the mass-flux fluctuations for x = 91.4 mm and y = 39 mm.

tices can intermittently thrust the high-momentum fluid from the outer part of the boundary layer down toward the wall, and vice versa. Secondly, spanwise vortices can produce a similar type of mixing as they convect downstream. In fact, a vortex sheet with quasiperiodic roll-up was observed by Ardonceau[12] and appeared to emerge and convect downstream from the foot of the oscillating shock. For the present 24-deg compression corner flow, a similar but aperiodic feature was seen in flow visualization and may be caused by instabilities associated with the inflectional mean velocity profiles observed downstream of the interaction.

If large-scale Taylor-Görtler or spanwise vortices are important mechanisms for turbulence amplification, then the turbulence amplification probably would be independent of the unsteady shock and the shock-induced separation and depend instead on the type and amount of turning or curvature. In light of this, the role of the unsteadiness of the shock in producing large turbulence amplification needs to be more closely examined, especially since previous work has suggested that unsteadiness may be an important mechanism.[11,26,27]

The energy spectra of the nondimensionalized mass-flux fluctuations for x = 91.4 mm are shown in Fig. 12. Above the boundary layer for x = 91.4 mm and $y \approx$ 39 mm, the hot wire

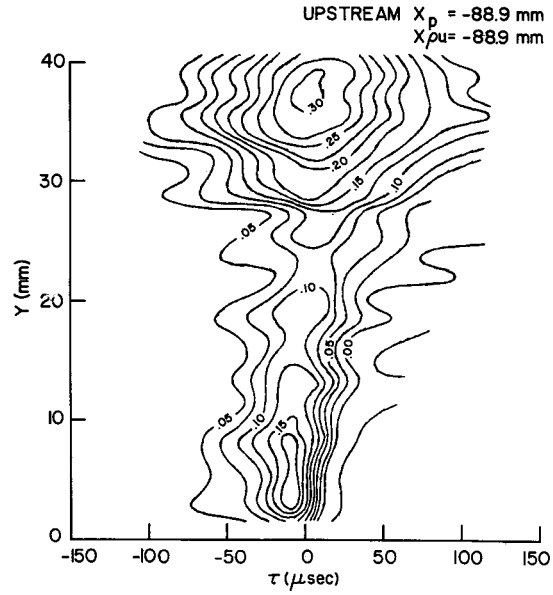

Fig. 14 Isocontours of the upstream mass-flux/wall-pressure space-time correlation coefficient $[p'(x_p,y=0,t)\rho U'(x_{\rho U},y,t-\tau)/\langle p'\rangle\langle \rho U'\rangle]$: x_p = − 88.9 mm and $x_{\rho U}$ = − 88.9 mm.

is in the region of the unsteady shock. A typical time history of the mass flux is shown in Fig. 13, clearly illustrating the jump in the mass flux across the shock. At this location, the spectrum is dominated by frequencies below 6 kHz with a maximum near 1 kHz, very much like the wall-pressure spectra at the foot of the shock. The expectation is that the low-frequency shock oscillations in the freestream would produce low-frequency fluctuations in the mass flux between the boundary-layer edge and the shock; however, this is not observed in the spectra. A similar result was found by Debieve and Lacharme[29] in their experimental study of freestream turbulence interacting with an unsteady shock. Their results showed that the upstream turbulence spectra were very much like the downstream, even though in the region of the shock a large amount of low-frequency energy was found in the spectra.

Within the boundary layer, the maxima in the spectra are located near 10 kHz, which again does not compare with the low-frequency shock motion. Contrary to this result, Ardonceau et al.[13] found for a separated 18-deg compression corner two broad peaks in the downstream spectra. One peak closely resembled the peak observed in the present flow—a high-frequency peak above the dominant unsteady shock frequency present throughout the boundary level. A second peak appeared near the wall (for $y < 0.5\delta_0$, where $\delta_0 \approx 8$ mm) at low frequencies believed to be characteristic of the low-frequency fluctuations of the separated region. No such low-frequency peak was observed in the present flow. Perhaps these differences are related to the flow regimes that were studied. In the present study, Re_{∞_0}/l was 5.9 times larger, and Re_{δ_0} was 17 times larger than that of Ardonceau. At least for the flow studied here, our results support the conclusion made earlier that the unsteadiness of the shock has little direct impact on the downstream turbulence.

Wall-Pressure/Mass-Flux Correlations

Isocontours of the mass-flux/wall-pressure space-time correlation coefficients are shown for the upstream and downstream boundary layer in Figs. 14 and 15. For both cases, the hot-wire probe was located at the same x station as the wall-pressure transducer. [With a small streamwise spacing between the hot-wire probe and the wall-pressure transducer (separation distances less than about 12.7 mm), similar trends were observed.[19]] Generally, the correlation is low everywhere. Near the separated zone (for which no figures are given), the corre-

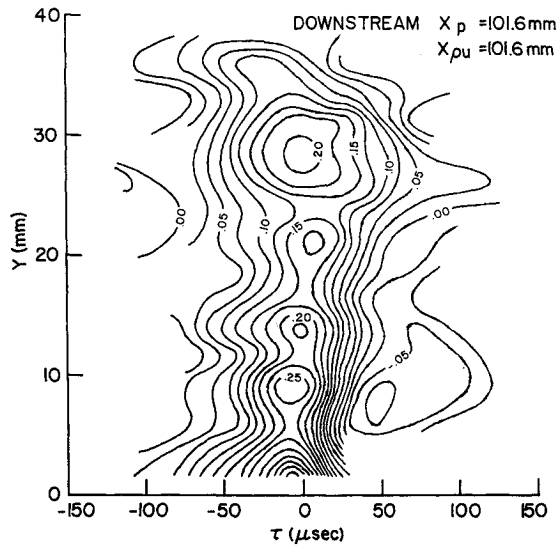

Fig. 15 Isocontours of the downstream mass-flux/wall-pressure space-time correlation coefficient $[p'(x_p,y=0,t)\rho U'(x_{\rho U},y,t-\tau)/\langle p'\rangle\langle \rho U'\rangle]$: $x_p = 101.6$ mm and $x_{\rho U} = 101.6$ mm.

lation is virtually zero for all y values. Very near the wall, correlation levels are expected to be higher simply because the pressure transducer signal arises mainly from near-wall motions (in the absence of wave-like disturbances produced by tunnel noise and shock motions).[16]

Despite the small correlation levels away from the wall, some comments can be made. Above the boundary layer a relatively large peak is present (0.30 correlation upstream), and this decreases by 30% downstream. The cospectra (not shown) in the region *above* the boundary layer show a high correlation level for frequencies below 3 kHz and practically no correlation at higher frequencies. Apparently, low-frequency fluctuations in the freestream mass-flux are strongly correlated with the wall static pressure fluctuations. It seems therefore that the correlations are dominated by the low-frequency noise in the wind tunnel. Even within most of the boundary layer, the cospectra show a high correlation level for frequencies below 3 kHz; however, there is a small level of correlation at higher frequencies. It seems that in the boundary layer (away from the near-wall region) the correlation must largely be due to tunnel noise, but the large-scale boundary-layer structures also make a contribution. Unfortunately, there is no way to discriminate between the wind-tunnel noise and the large-scale structures.

Other trends to note for the correlation in the boundary layer are the following: 1) as expected the correlation decreases with distance from the wall; 2) in contrast to the correlation outside the boundary layer, the correlation inside the boundary layer increases downstream; 3) the correlation shows a peculiar family of peaks; and 4) the time delay for maximum correlation increases with distance from the wall.

Boundary-Layer Intermittency

A conditional sampling analysis was applied to the mass-flux signal to detect the intermittent behavior of the outer part of the boundary layer. A hybrid algorithm for this interface statistic was developed by combining the VITA technique[30] and a "threshold level" condition of the mass-flux signal. Note that in this application the VITA technique was not used to detect turbulent events within the boundary layer but instead was adapted for turbulent/nonturbulent detection

First, it was necessary to take account of the freestream turbulence intensity. Hence, the short-time variance of the mass flux outside the boundary layer was used, and it was computed according to

$$\sigma_0 = \left(\frac{1}{\tau}\right)\int_{t-\tau/2}^{t+\tau/2} [\rho U(t)]^2\, dt - \left[\frac{1}{\tau}\int_{t-\tau/2}^{t+\tau/2} \rho U(t)\, dt\right]^2 \quad (1)$$

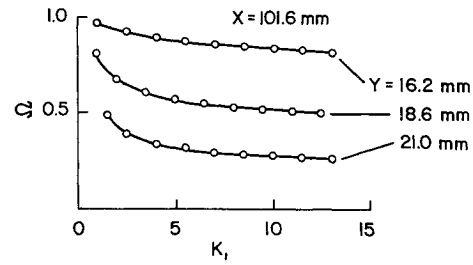

Fig. 16 Variation of the downstream boundary-layer intermittency with K_1.

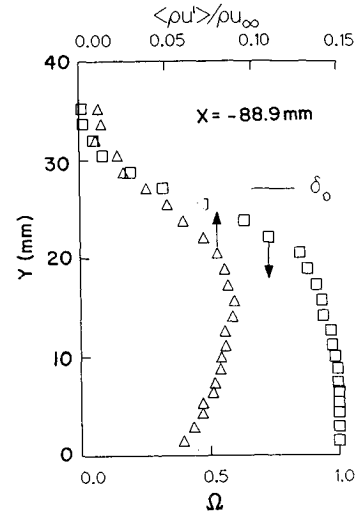

Fig. 17 Intermittency of the upstream boundary layer; the turbulence intensity profile is shown for reference: □, Ω, Δ, $\langle(\rho u)'\rangle/\rho U$.

Then the average of this outer variance was defined by

$$\overline{\sigma_0(t)} = \lim_{T\to\infty}\left(\frac{1}{T}\right)\int_0^T \sigma_0(t,\tau)\, dt \quad (2)$$

The beginning of the intermittency within the boundary layer was taken to occur when

$$\sigma(t,\tau) > K_1\overline{\sigma_0(\tau)} \quad (3)$$

and the ending was given by

$$\sigma(t,\tau) < K_1\overline{\sigma_0(\tau)} \quad (4a)$$

$$(\rho U)(t) > K_2(\rho U)_\infty \quad (4b)$$

where $\sigma(t,\tau)$ is the short-time variance within the boundary layer. The intermittency Ω then was defined as the total time of intermittency divided by the total time T, that is,

$$\Omega = \left(\sum_{i=0}^{N} t_i\right)/T \quad (5)$$

The intermittency was not especially sensitive to the mass-flux threshold constant K_2. In contrast, K_1 had to be chosen carefully. For $K_2 = 0.75$ and $\tau = 24$ μs, Fig. 16 shows the variation of the intermittency with K_1 at a fixed station downstream of the corner. From these results and by inspection of the individual time histories, K_1 was selected to be 10, where the intermittency is nearly independent of K_1. Generally, the same result was found for the upstream boundary layer. The intermittency of the upstream boundary layer based on these threshold values is shown in Fig. 17. It appears that the intermittency of the outer edge of the supersonic boundary layer is less than in the subsonic case, in agreement with the results by

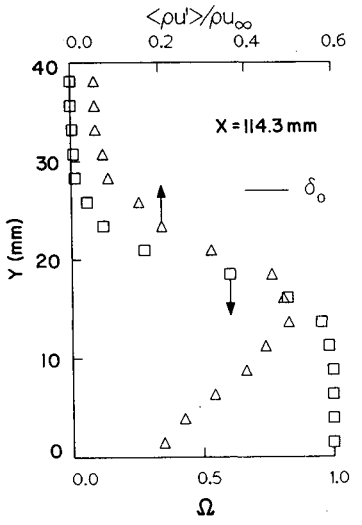

Fig. 18 Intermittency of the downstream boundary layer; the turbulence intensity profile is shown for reference: □, Ω, Δ, $<(\rho u)'>/\rho U$.

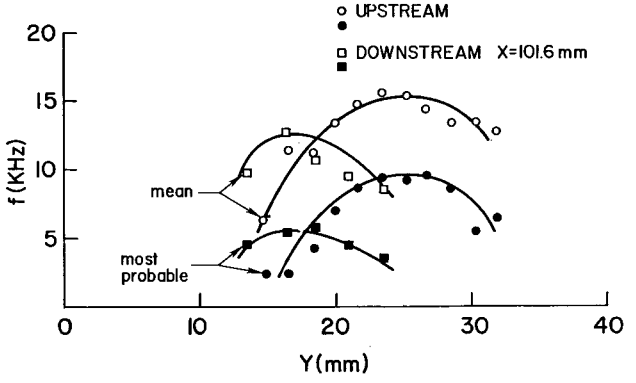

Fig. 19 Most probable and mean frequencies of the upstream and downstream boundary-layer intermittency.

Owen et al.[31] in a hypersonic turbulent boundary layer, although the differences in the present case are rather small. As for the downstream boundary-layer intermittency (see Fig. 18), the intermittency falls off faster than in the upstream case. In Fig. 19, the frequency of the intermittency is shown for the upstream and downstream boundary layers. Interestingly, the most probable and mean frequencies of the upstream boundary layer are smaller than the downstream by a factor of 2. It seems clear that the boundary-layer structure changes significantly in passing through the interaction, in a manner consistent with the appearance of large-scale motions bringing freestream fluid deep into the boundary level.

Conclusions

In this experimental investigation, the flow over a 24-deg compression corner was examined. In agreement with previous studies, the flow was found to be highly unsteady with random broadband large-scale shock oscillations at 1.5–2 kHz as deduced from wall-pressure spectra at the foot of the shock. Through the interaction, the maximum mass-flux turbulence intensity within the boundary layer is amplified by a factor of about 5 over that of the upstream level, even though the mean mass flux increases by only a factor of 2. It has been widely held that a large fraction of the turbulence amplification is caused by unsteady shock motion; however, no direct effects of unsteady shock motion were observed in the downstream turbulence properties. Furthermore, the shock-wave unsteadiness and the downstream boundary layer do not appear to be significantly affected by the large shock-induced separated region. It was observed that the pdf's of the upstream boundary-layer turbulence are characterized by Gaussian-type distributions, whereas in the downstream boundary layer the pdf's are bimodal, centering about two distinct levels, one representative of the freestream mass flux and one representation of a lower level found near the wall. The boundary-layer intermittency results showed that the frequency of the intermittency decreased through the interaction, and this too suggests changes in the boundary-layer structure. In light of this, the upstream and the downstream boundary layers must be fundamentally different. Since the mean velocity profiles downstream are inflectional, they may give rise to spanwise "vortices" like those observed in the mixing layer between two unequal parallel jets.[32] Such large-scale lateral structure could produce the type of mixing observed. Unsteady streamwise Taylor-Görtler type vortices also may play an important role in bringing low-speed momentum fluid up from the wall and high-speed momentum fluid down from the freestream. Given that the upstream and downstream boundary layers are fundamentally different, it is unlikely that turbulence models that work successfully for the well-behaved upstream boundary layer will work equally well for downstream boundary layer. The different nature of the downstream boundary layer needs to be taken into account in turbulence modeling for these unsteady interaction flows.

Acknowledgments

This research was supported by the Army Research Office under Contract DAAG29-85-K-0255 monitored by Dr. R. Singleton and Dr. T. Doligalski.

References

[1]Horstman, C. C., Settles, G. S., Vas, I. E., Bogdonoff, S. M., and Hung, C. M., "Reynolds Number Effects on Shock Wave Turbulent Boundary-Layer Interactions," *AIAA Journal,* Vol. 15, Aug. 1977, pp. 1152–1158.

[2]Coakley, T. J., Viegas, J. R., and Horstman, C. C., "Evaluation of Turbulence Models for Three Primary Type of Shock Wave/Boundary Layer Interactions," AIAA Paper 77-692, June 1977.

[3]Marvin, J. G., "Turbulence Modeling for Computational Aerodynamics," *AIAA Journal,* Vol. 21, July 1983, pp. 941–995.

[4]Visbal, M. and Knight, D. D., "The Baldwin-Lomax Turbulence Model for Two-Dimensional Shock Wave Boundary Layer Interactions," *AIAA Journal,* Vol. 22, July 1984, pp. 921–928.

[5]Settles, G. S., Vas, I. E., and Bogdonoff, S. M., "Details of a Shock-Separated Turbulent Boundary Layer at a Compression Corner," *AIAA Journal,* Vol. 14, Dec. 1976, pp. 1709–1715.

[6]Dolling, D. S. and Murphy, M.T., "Unsteadiness of the Separation Shock Wave in a Supersonic Compression Ramp Flowfield," *AIAA Journal,* Vol. 21, Dec. 1983, pp. 1628–1634.

[7]Dolling, D. S. and Or, C. T., "Unsteadiness of the Shock Wave Structure in Attached and Separated Compression Corner Flowfields," AIAA Paper 83-1715, July 1983.

[8]Dussauge, J. P., Muck, K. C., and Andreopoulos, J., "Properties of Wall Pressure Fluctuations in a Separated Flow over a Compression Ramp," *Turbulent Shear-Layer/Shock Wave Interactions,* edited by J. Délery, Springer-Verlag, Berlin, 1986, pp. 383–392.

[9]Andreopoulos, J. and Muck, K. C., "Some New Aspects of the Shock Wave Boundary-Layer Interaction in Compression Ramp Flows," *Journal of Fluid Mechanics,* Vol. 180, July 1987, pp. 405–428; see also AIAA Paper 86-0342, Jan. 1986.

[10]Narlo, J. C., "Experimental Investigation of the Driving Mechanism of Separation Shock Wave Motion in Interaction Flows," M. S. Thesis, Univ. of Texas at Austin, Austin, TX, 1986.

[11]Smits, A. J. and Muck, K. C., "Experimental Study of Three Shock Wave/Turbulent Boundary-Layer Interactions," *Journal of Fluid Mechanics,* Vol. 182, Sept. 1987, pp. 291–314.

[12]Ardonceau, P. L., "The Structure of Turbulence in a Supersonic Shock-Wave/Boundary Layer Interaction," *AIAA Journal,* Vol. 22, Sept. 1984, pp. 1254–1262.

[13]Ardonceau, P. L., Lee, D. H., Roquefort, T. A., and Goethals, R., "Turbulence Behavior in a Shock Wave/Boundary Layer Interaction," AGARD-CP-271, 1978.

[14]Samimy, M., Petrie, H. L., and Addy, A. L., "A Study of Compressible Turbulent Reattaching Free Shear Layer," *AIAA Journal,* Vol. 24, Feb. 1986, pp. 261–267.

[15]Taylor, M. W., "A Supersonic Turbulent Boundary Layer on Concavely Curved Surfaces," M.S.E. Thesis, Dept. of Mechanical and Aerospace Engineering, Princeton Univ., Princeton, NJ, 1984.

[16]Spina, E. F. and Smits, A. J., "Organized Structures in Compressible Turbulent Boundary Layers," *Journal of Fluid Mechanics,* Vol. 182, Sept. 1987, pp. 85–109.

[17]Smits, A.J., Muck, K. C., and Hawakawa, K., "Constant Temperature Hot-Wire Anemometer Practice in Supersonic Flows, Part I – The Normal Wire," *Experiments in Fluids,* Vol. 1, Springer-Verlag, 1983, pp. 83–92.

[18]Watmuff, J. H., "Some Higher-Order Effects in the Behavior of Constant Temperature Hot-Wire Anemometer Systems," *ASME Conference on Thermal Anemometry,* edited by D. E. Stock, American Society of Mechanical Engineers, New York, June 1987, pp. 25–34.

[19]Selig, M. S., "Unsteadiness of Shock Wave/Turbulent Boundary-Layer Interactions with Dynamic Control," M.S.E. Thesis, Dept. of Mechanical and Aerospace Engineering, Princeton Univ., Princeton, NJ, 1988.

[20]Settles, G. S., "An Experimental Study of Compressible Turbulent Boundary-Layer Separation at High Reynolds Numbers," Ph.D. Dissertation, Dept. of Aerospace and Mechanical Sciences, Princeton Univ., Princeton, NJ, 1975.

[21]Settles, G. S., Fitzpatrick, T. J., and Bogdonoff, S. M., "Detailed Study of Attached and Separated Compression Corner Flowfield in High Reynolds Number Supersonic Flow," *AIAA Journal,* Vol. 17, June 1979, pp. 579–585.

[22]Donovan, J. F. and Smits, A. J., "A Preliminary Investigation of Large-Scale Organized Motions in a Supersonic Turbulent Boundary Layer on a Curved Surface," AIAA Paper 87-1285, June 1987.

[23]Fernholz, H. H. and Finley, P. J., "A Critical Commentary on Mean Flow Data for Two-Dimensional Compressible Turbulent Boundary Layers," AGARDograph No. 253, 1980.

[24]Settles, G. S., Perkins, J. J., and Bogdonoff, S. M., "Upstream Influence Scaling of 2D & 3D Shock/Turbulent Boundary Layer Interactions at Compression Corners," AIAA Paper 81-0334, Jan. 1981.

[25]Kuntz, D. W., Amatucci, V. A., and Addy, A. L., "Turbulent Boundary-Layer Properties Downstream of a Shock-Wave/Boundary-Layer Interaction," *AIAA Journal,* Vol. 25, May 1987, pp. 668–675.

[26]Zang, T. A., Hussaini, M. Y., and Bushnell, D. M., "Numerical Computations of Turbulence Amplification in Shock-Wave Interactions," *AIAA Journal,* Vol. 22, Jan 1984, pp.13–21.

[27]Hussaini, M. Y., Collier, F., and Bushnell, D. M., "Turbulence Alteration Due to Shock Motion," *Turbulent Shear-Layer/Shock-Wave Interactions,* edited by J. Délery, Springer-Verlag, Berlin, 1986, pp. 371–381.

[28]Hayakawa, K., Smits, A. J., and Bogdonoff, S. M., "Turbulence Measurements in a Compressible Reattaching Shear Layer," *AIAA Journal,* Vol. 22, July 1984, pp. 889–895.

[29]Debieve, J. F. and Lacharme, T. P., "A Shock-Wave/Free Turbulence Interaction, *Turbulent Shear-Layer/Shock-Wave Interactions,* edited by J. Délery, Springer-Verlag, Berlin, 1986, pp. 393–403.

[30]Blackwelder, R. F. and Kaplan, R. E., "On Wall Structure of the Turbulent Boundary Layer," *Journal of Fluid Mechanics,* Vol. 76, July–Aug. 1976, pp. 89–112.

[31]Owen, F. K., Horstman, C. C., and Kussoy, M. I., "Mean and Fluctuating Flow Measurements of a Fully-Developed Non-Adiabatic Hypersonic Boundary Layer," *Journal of Fluid Mechanics,* Vol. 70, July–Aug. 1975, pp. 393–413.

[32]Brown, G. L. and Roshko, A., "On Density Effects and Large-Scale Turbulent Mixing Layers," *Journal of Fluid Mechanics,* Vol. 64, June–July 1974, pp. 775–816.